Tayronne de Almeida Rodrigues
João Leandro Neto
Dennyura Oliveira Galvão
(Organizadores)

MEIO AMBIENTE, SUSTENTABILIDADE E AGROECOLOGIA 5

Atena Editora
Ano 2019

Tayronne de Almeida Rodrigues
João Leandro Neto
Dennyura Oliveira Galvão
(Organizadores)

Meio Ambiente, Sustentabilidade e Agroecologia 5

Atena Editora
2019

2019 *by Atena Editora*

Editora Chefe: Profª Drª Antonella Carvalho de Oliveira
Diagramação e Edição de Arte: Lorena Prestes e Geraldo Alves
Revisão: Os autores

Dados Internacionais de Catalogação na Publicação (CIP)
(eDOC BRASIL, Belo Horizonte/MG)

M514 Meio ambiente, sustentabilidade e agroecologia 5 [recurso eletrônico] / Organizadores Tayronne de Almeida Rodrigues, João Leandro Neto, Dennyura Oliveira Galvão. – Ponta Grossa (PR): Atena Editora, 2019. – (Meio Ambiente, Sustentabilidade e Agroecologia; v. 5)

Formato: PDF
Requisitos de sistema: Adobe Acrobat Reader
Modo de acesso: World Wide Web
Inclui bibliografia
ISBN 978-85-7247-331-6
DOI 10.22533/at.ed.316191604

1. Agroecologia – Pesquisa – Brasil. 2. Meio ambiente – Pesquisa – Brasil. 3. Sustentabilidade. I. Rodrigues, Tayronne de Almeida. II.Leandro Neto, João. III. Galvão, Dennyura Oliveira. IV. Série.
CDD 630

Elaborado por Maurício Amormino Júnior – CRB6/2422

APRESENTAÇÃO

A obra Meio Ambiente, Sustentabilidade e Agroecologia vem tratar de um conjunto de atitudes, de ideias que são viáveis para a sociedade, em busca da preservação dos recursos naturais.

Em sua origem a espécie humana era nômade, e vivia integrada a natureza, sobreviviam da caça e da colheita. Ao perceber o esgotamento de recursos na região onde habitavam, migravam para outra área, permitindo que houvesse uma reposição natural do que foi destruído. Com a chegada da agricultura o ser humano desenvolveu métodos de irrigação, além da domesticação de animais e também descobriu que a natureza oferecia elementos extraídos e trabalhados que podiam ser transformados em diversos utensílios. As pequenas tribos cresceram, formando cidades, reinos e até mesmo impérios e a intervenção do homem embora pareça benéfica, passou a alterar cada vez mais negativamente o meio ambiente.

No século com XIX as máquinas a vapor movidas a carvão mineral, a Revolução Industrial mudaria para sempre a sociedade humana. A produção em grande volume dos itens de consumo começou a gerar demandas e com isso a extração de recursos naturais foi intensificada. Até a agricultura que antes era destinada a subsistência passou a ter larga escala, com cultivos para a venda em diversos mercados do mundo. Atualmente esse modelo de consumo, produção, extração desenfreada ameaça não apenas a natureza, mas sua própria existência. Percebe-se o esgotamento de recursos essenciais para as diversas atividades humanas e a extinção de animais que antes eram abundantes no planeta. Por estes motivos é necessário que o ser humano adote uma postura mais sustentável.

A ONU desenvolveu o conceito de sustentabilidade como desenvolvimento que responde as necessidades do presente sem comprometer as possibilidades das gerações futuras de satisfazer seus próprios anseios. A sustentabilidade possui quatro vertentes principais: ambiental, econômica, social e cultural, que trata do uso consciente dos recursos naturais, bem como planejamento para sua reposição, bem como no reaproveitamento de matérias primas, no desenvolvimento de métodos mais baratos, na integração de todos os indivíduos na sociedade, proporcionando as condições necessárias para que exerçam sua cidadania e a integração do desenvolvimento tecnológico social, perpetuando dessa maneira as heranças culturais de cada povo. Para que isso ocorra as entidades e governos precisam estar juntos, seja utilizando transportes alternativos, reciclando, incentivando a permacultura, o consumo de alimentos orgânicos ou fomentando o uso de energias renováveis.

No âmbito da Agroecologia apresentam-se conceitos e metodologias para estudar os agroecossistemas, cujo objetivo é permitir a implantação e o desenvolvimento de estilos de agricultura com maior sustentabilidade, como bem tratam os autores desta obra. A agroecologia está preocupada com o equilíbrio da natureza e a produção de alimentos sustentáveis, como também é um organismo vivo com sistemas integrados

entre si: solo, árvores, plantas cultivadas e animais.

Ao publicar esta obra a Atena Editora, mostra seu ato de responsabilidade com o planeta quando incentiva estudos nessa área, com a finalidade das sociedades sustentáveis adotarem a preocupação com o futuro.

Tenham uma excelente leitura!

Tayronne de Almeida Rodrigues
João Leandro Neto
Dennyura Oliveira Galvão

SUMÁRIO

CAPÍTULO 31

EXPERIMENTAL VARIABLES IN THE SYNTHESIS OF TIO_2 NANOPARTICLES AND ITS CATALYTIC ACTIVITY

Thalles Moura Fé Marques
Federal Institute of Education, Science and Technology of Piauí, Teresina – PI, and Federal University of Piauí, Campus Minister Petrônio Portela, Teresina - PI, Brazil.

Juliana Sousa Gonçalves
Federal University of Piauí - Department of Chemical, Campus Minister Petrônio Portela, Teresina - PI

Valdemir dos Santos
Federal University of São Carlos - Department of Chemical, São Carlos - SP.

Francisco Xavier Nobre
Federal Institute of Amazonas, Campus Coari. Coari – AM.

Bartolomeu Cruz Viana Neto
Federal University of Piauí – Department of Physics, Campus Minister Petrônio Portela, Teresina - PI

José Milton Elias de Matos
Federal University of Piauí- Department of Chemical, Campus Minister Petrônio Portela, Teresina - PI

ABSTRACT: Nanoparticles of titanium dioxide ($TiO_{2)}$ (average size ~ 5 – 579 nm) with a high surface area (~ 192 $m^2 g^{-1}$) were synthesized in the pure anatase phase, either with or without $H_2O_{2,}$ using isopropanol or acetic acid as a reaction medium. TiO_2 was characterized by using XRD, BET surface area, STEM and UV-Visible techniques. TiO_2 was obtained differed according to the reaction medium used. Bandgap energy values observed for TiO_2 with H_2O_2 were 3.10 for TiO_2 with IP, and 2.97 for TiO_2 with HAc. Values when H_2O_2 was not used were 3.07 for TiO_2 obtained with IP and 3.40 with HAc. The catalytic activity of TiO_2 in solutions of H_2O_2 was studied by examining the decolorization of methylene blue in the dark. The decolorization in the presence of pretreated TiO_2 of approximately 100% was obtained within 7h in the presence of TiO_2 obtained in HAc and presence of H_2O_2.
KEYWORDS: *Hydrogen peroxide, solvothermal method, titania nanocrystals.*

1 I INTRODUCTION

Titanium dioxide (titania - TiO_2) is used in different environmental applications, such as photocatalytic degradation for purification of polluted air and in wastewater treatment [CARP; HUISMAN; RELLER, 2004; LI et all., 2003; GARCIA-SEGURA; BRILLAS, 2017, PUEYO et all., 2016]. It also has a wide variety of technological applications, such as pigments, wet-type solar cells [MICHAEL, 2001; AHMAD; PANDEY; RAHIM, 2017], sensors [HIROSHI et all., 2005, ZHANG et all., 2017], photocatalysts [ZHANG et all., 2017, BORA, MEWADA, 2017] and electronic material [LI et all., 2003, DAIA et

all., 2003].

There are three main crystallographic forms of TiO_2: rutile (tetragonal), anatase (tetragonal), and brookite (orthorhombic) [LI; WHITE; LIM, 2003, Y. HU; TSAI; HUANG, 2003]. Rutile is thermodynamically stable and the other two forms are metastable [GOPAL; CHAN; DE JONGHE, 1997]. The anatase form has been used in photocatalysis and various other applications [ZAKRZEWSKA; RADECKA, 2017, LOAN et all., 2017].

Methods of synthesizing anatase TiO_2 crystals and anatase TiO_2 mesocrystals have been extensively described in scientific literature, including the sol–gel method [PACHECO et all., 2004], the precipitation method [GOPAL; CHAN; DE JONGHE, 1997], aerosol synthesis [AHONEN et all., 2001], and the hydrothermal method [KARTHIKEYAN et all, 2017, BOKHIMI; PEDRAZA, 2004]. In some of these processes, preparation costs can be high, the reaction is time consuming and the process is complex. In order to obtain ultrafine particles, milling and thermal treatment are also needed. In the hydrothermal method, the reaction conditions, such as solution concentration, temperature and pH, have a strong influence on the reaction process but it is relatively easy to control, and the cost is low. Some of the advantages of the hydrothermal method over other fabrication techniques include the purity, homogeneity, and stoichiometry control of the particles obtained. The size of TiO_2 particles produced depends upon the grain size and composition, but not on the calcination temperature.

However, anatase TiO_2 crystals or mesocrystals usually prepared by the methods cited above require either complex processing steps or high energy consumption. Some of these methods can be unfavourable for practical and commercial applications in the industry. Goutailler et al. synthesized photocatalytic active nanoparticulate TiO_2 at a low temperature (100 °C) by an aqueous sol–gel method, but ammonium bromide salts were needed as catalysts [GOUTAILLER et all., 2002]. Hao *et al*. obtained mesoporous titania powder with a mixture of phase (anatase and brookite) framework at low temperatures (80–100 °C) by a modified sol–gel method using dodecylamine as a template [HAO; ZHANG, 2008]. Serrano *et al*. [LI et all., 2017] prepared micro-mesoporous TiO_2 photocatalysts by a mild crystallization procedure (40 °C), using in the crystallization step four inorganic acids in the refuxing treatment. In this same way Li *et al*. prepared anatase TiO_2 mesocrystals at low temperature (80 °C) in one-pot synthesis *via* acetic acid (HAc)-induced hydrolysis [LI et all., 2017].

Various parameters such as pH, presence/absence of catalyst, temperature, chelating reagent, nature of precursor, use of organic acid or H_2O_2 influence the size, shape and phase of TiO_2 [SUGIMOTO; ZHOU; MURAMASTU, 2003a, SUGIMOTO; ZHOU; MURAMASTU, 2003b, ATTAR et all., 2008, CHANG et all., 2009]. Chang *et al*. have investigated the effect of pH on the phase and morphology evolution of nano TiO_2 from peroxo titanium complex in the presence of HAc as chelating agent [CHANG et all., 2009]. Sugimoto *et al*. have studied the influence of pH on the size control and various amines on the shape control of anatase TiO_2 prepared from sol–gel process [SUGIMOTO; ZHOU; MURAMASTU, 2003a, SUGIMOTO; ZHOU; MURAMASTU,

2003b]. Attar *et al*. have reported the effect of modifier ligands (HAc and acetyl acetone) on the nano TiO_2 formation from TIP by sol–gel method [ATTAR et all., 2008].

HAc is considered to play a key role during the formation of TiO_2 mesocrystals, promoting the transformation of TiO_2 from the amorphous state to the anatase phase at low temperatures (80 °C). The morphology and size of the mesocrystals of TiO_2 anatase prepared in the presence of HAc can be adjusted continuously in the range of 20 nm to 100 nm, adjusting the concentration of HAc [LI et all., 2017, PARRA et all., 2008].

Compared to the hydrothermal method for obtaining TiO_2, the wet chemical route using the peroxo titanium complex has been little explored [CHANG et all., 2010]. Although some systems have previously investigated. But even not being much explored the peroxide-based route for synthesizing titanium oxide powder is well established [ATTAR et all., 2008, CHANG et all., 2010, MUHLEBACH; MULLER; SCHWARZENBACH, 1970, GAO et all., 2003, GAO; MASUDA; KOUMOTO, 2004, GAO et all., 2007, GAO et all., 2008, JAGADALE et all., 2008].

This study described the synthesis of titanium dioxide nanoparticles which were obtained using the peroxide method. Pure anatase was obtained by the hydrothermal method in the presence of hydrogen peroxide (H_2O_2) using solutions of titanium tetraisopropoxide in isopropanol (IP) or acetic acid (HAc). Hydrogen peroxide is an ideal environmentally friendly solvent and oxidant and used widely to the synthesis of nanostructures of inorganic materials [LI et all., 2006]. The catalytic activity of TiO_2 in solutions of H_2O_2 was studied by examining the decolorization of methylene blue in the dark.

2 | EXPERIMENTAL PROCEDURE

2.1 Titania nanoparticles synthesis

Titania nanoparticles (TiO_2) were synthesized using three methods: *Method A*: by mixing 2.5 mL of titanium isopropoxide (TIP, $Ti[OCH(CH_3)_2]_4$, > 99%, Acros Organics) in 50 mL of isopropanol (IP, 99.5%, Vetec) or Acetic Acid (HAc, 99.5%, Vetec). The solution was poured into an autoclavable bottle. The bottle was then placed in a regular laboratory oven at a constant 100 °C for 48h.

Method B: by mixing 2.5 mL of titanium isopropoxide and 8 mL of hydrogen peroxide (H_2O_2 10% V/V, > 99%, Acros Organics), was dissolved in 50 mL of isopropanol. The solution was poured into an autoclavable bottle. The bottle was then placed in a regular laboratory oven at a constant 100 °C for 48h.

Method C: TiO_2 was obtained by mixing 2.5 mL of TIP and 8 mL of H_2O_2, which was dissolved in 50 mL of Acetic Acid. The solution was poured into an autoclavable bottle. The bottle was then placed in a regular laboratory oven at a constant 100 °C for 48h. A gel was formed and it was hydrolyzed by adding 50 mL of milliq water. The bottle

was then placed again in the oven at a constant 100 °C for 24h.

2.2 Characterizations

X-Ray diffraction patterns were carried out with a Rigaku diffractometer, D-Max 2500 2500PC, Japan with Cu Kα radiation in the 2θ range from 5° to 75° in a continuous scan of 0.02°/min, CuKa radiation. Measurements of the surface area, hysteresis curve, and pore size distribution of the TiO_2 samples were obtained by nitrogen adsorption/desorption analysis. A Gaussian function was used to fit the pore size distribution curve. For the HRTEM/TEM (200 kV, model CM200; Philips, Holland) study, a drop of the powder suspension was deposited on a carbon-covered nickel grid. The Raman and infrared spectra were obtained using a Bruker RFS-100/S Raman spectrometer and Bruker Equinox-55. UV–vis spectroscopy for the spectra of optical absorbance in disordered and crystalline TiO_2 powders was taken using Cary 5G equipment. All measurements in this work were taken at room temperature.

2.3 Decolorization of methylene blue

A solution of 0.5 mM methylene blue was prepared and used in this study. The decolorization of methylene blue was first examined in the presence of pretreated TiO_2. TiO_2 powder (50 mg) was incubated in a 110-mM H_2O_2 solution (10 mL) in the dark. The suspension was then centrifuged at 5000 rpm for 10 min. All solutions were incubated in the dark with agitation. After this process solutions were analyzed according to the change of time, which was measured with a spectrophotometer (Cary 300) at 661 nm.

3 I RESULTS AND DISCUSSION

In this work, it was shown that TiO_2 nanocrystal formation in a highly crystalline phase is strongly dependent on the reaction medium. An increase of crystallinity of the anatase phase of TiO_2 was observed when isopropanol (IP) was replaced by acetic acid (HAc) (as reaction medium), and did not depend upon whether H_2O_2 was used or not. With IP, the reaction occurs faster than with HAc. With IP, a nanocrystalline powder (anatase) was obtained as a solid in a solution of IP after 48h of reaction (at 100 °C). However, after 48h of reaction with HAc (at 100 °C), the solution turned into a gel, and hydrolysis occurred after the addition of water. The bottle was then placed in the oven at a constant 100 °C for a further 24h. In this case, the hydrolysis rate occurred slowly, which increased the crystallinity of TiO_2.

The same procedure was carried out to obtain TiO_2 in the presence of IP or HAc, but without H_2O_2. The aim of these syntheses was to compare the formed products and discover the real role of H_2O_2 and whether the solutions had the same behavior as when H_2O_2 was used.

Fig. 1 shows the patterns of X-ray diffraction of the synthesized TiO_2 samples

obtained in presence and absence of H_2O_2. Fig. 1 (a and b) shows the patterns of X-ray diffraction of the synthesized TiO_2 samples beginning with titanium isopropoxide, then hydrogen peroxide, isopropanol and acetic acid.

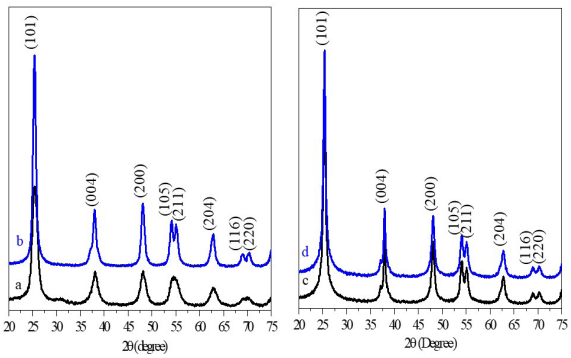

Figure 1. XRD patterns of TiO_2 obtained in the presence of H_2O_2 using (a) isopropanol and (b) acetic acid and in absence of H_2O_2 using (c) isopropanol and (d) acetic acid, as reaction medium.

No peaks corresponding to the rutile or brookite phases were observed, which indicates that the TiO_2 powders obtained had a monophasic anatase structure (PDF #21-1272 anatase TiO_2). The crystal structure of the TiO_2 powders was not affected by changing the reaction medium. The narrow diffraction peaks suggest that the TiO_2 that was obtained was nano sized. The average crystalline sizes of anatase phase TiO_2 particles can be calculated by applying Scherrer's equation to the anatase (101) diffraction peak, as shown in Table 1.

	Sample	crystallite size (nm)[a]	Superficial area BET (m^2 g^{-1})	Porous volume (cm^3)	Porous size (nm)
With H_2O_2	**TiO_2 – IP**	10.12	192.81	0.46	9.56
	TiO_2 - HAc	12.16	157.89	0.29	7.34
Without H_2O_2	**TiO_2 – IP**	14.06	148.73	0.22	6.47
	TiO_2 - HAc	15.52	129.39	0.21	5.38

Table 1. Texture Data of TiO_2 samples.

[a] calculated using Scherrer's equation

TiO_2 obtained without H_2O_2 (Fig. 1 (c and d)) had the same profile as DRX (not shown). The TiO_2 that was obtained was identified as pure anatase TiO_2 (PDF #21-1272 anatase TiO_2) and, no peaks corresponding to any other phase were observed, which indicates that the obtained TiO_2 powders also exhibited a monophasic anatase structure. The average crystalline sizes were calculated by applying Scherrer's equation to the anatase (101) diffraction peak as shown in Table 1.

Changing the reaction medium from IP to HAc improved the crystallinity of TiO_2

powders (Fig. 1 and 2). However, the titania obtained without H_2O_2 had a low amount of amorphous titania. This is due to the fast hydrolysis of titanium salt, which results in a fast precipitation of TiO_2, and a powder with low crystallinity.

In order to further characterize the crystalline phase of the calcined TiO_2, FT-Raman measurement was performed. The pattern is shown in Fig. 2. The FT-Raman spectrum for TiO_2 obtained with H_2O_2 clearly shows a strong band at 148 cm^{-1} and four other bands at 200, 398, 516 and 638 cm^{-1} which arose from the optical vibration modes represented as $E_g(v_6)$, $E_g(v_5)$, $B_{1g}(v_4)$, A_{1g} +$B_{1g}(v_2 + v_3)$ and Eg(v1) [HAO; ZHANG, 2008]. They can be assigned the characteristic pattern for pure anatase without the presence of rutile or brookite phase [LIU et all., 2006], which is consistent with the XRD analysis.

The FT-Raman spectrum for TiO_2 obtained without H_2O_2 had a similar profile to the one with H_2O_2.

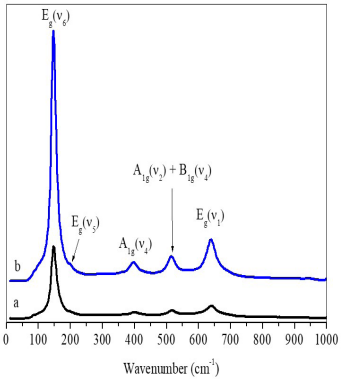

Figure 2. Raman spectra for TiO_2 (at room temperature) obtained in the presence of H_2O_2 using isopropanol (a) or acetic acid (b) as reaction medium.

The morphology and average size of the synthesized pure nanocrystalline anatase TiO_2 as a function of the reaction medium were investigated in detail using electronic microscopy (FEG-STEM). Fig. 3 shows the STEM micrographs of the anatase TiO_2 samples synthesized with hydrogen peroxide in isopropanol as reaction medium for a constant reaction time (48h) (Fig. 3a and 3b) and without H_2O_2 (Fig. 3c and 3d). The STEM images of all the samples show an irregular spherical shape (Fig. 3a) and rod-like structures were obtained in samples, both in the presence (Fig. 3b) and absence (Fig. 3a and 3b) of H_2O_2.

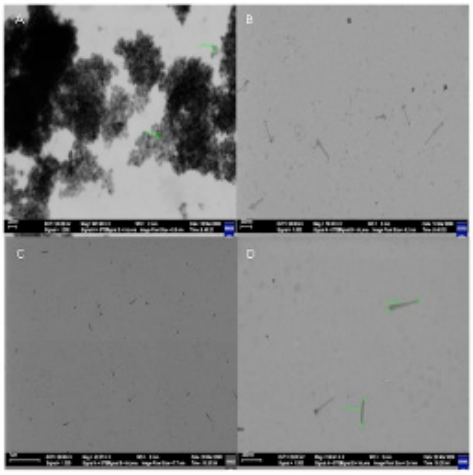

Figure 3. SEM images of TiO_2 samples obtained in the (a e b) presence and (c and d) absence of H_2O_2 and using isopropanol as reaction medium.

The irregular spherical nanocrystals are about 7 and 9 nm in diameter, as shown in Fig. 3a. The rods in the sample obtained with H_2O_2 are about 39 nm in diameter and 495 nm long, as shown in Fig. 3b. However, the diameters of the rods in the sample obtained without H_2O_2 are much smaller, reaching a maximum of about 27 nm and 156 nm long, as shown in Fig. 3(c and d). The crystallite shapes turn into nanorods with different sizes. We believe that the mechanisms of crystal growth are influenced by the presence of hydrogen peroxide. In its absence, the effect of the starting material can be explained as follows: The titanium salt is surrounded by a large amount of OH^- and the nucleation of $Ti(OH)_x$ is fast, whereas the particle growth is restricted by surrounding OH^-, which results in small $Ti(OH)_x$ crystallites. The freshly formed titanium hydroxide decomposes rapidly and thus TiO_2 nanocrystals are produced. In the presence of $H_2O_{2,}$ the starting material is titanium peroxide, the OH^- concentration around Ti^{4+} decreases, and the nucleation of $Ti(OH)_x$ slows down. As a result, the TiO_2 produced is more irregular in shape and much larger in size.

Fig. 4 shows the STEM micrographs of the anatase TiO_2 samples synthesized with hydrogen peroxide in acetic acid as reaction medium, for a constant reaction time (48h), and for an additional 24h (Fig. 4a and 4b). It also shows the same process when H_2O_2 is not used (Fig. 4c and 4d). The STEM images of all the samples have an irregular spherical shape (Fig. 4a and 4b), a rod-like shape (Fig. 4b) and nanotube structures were also obtained too (Fig. 4b). In the absence of H_2O_2, irregular rods were obtained (Fig. 4c and 4d).

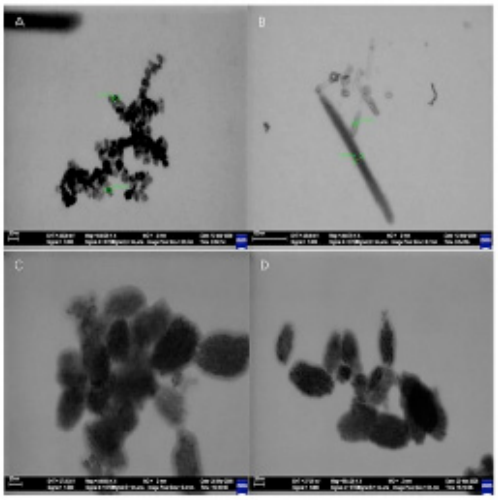

Figure 4. SEM images of TiO_2 samples obtained in the (a e b) presence and (c and d) absence of H_2O_2 and using acetic acid as reaction medium.

The irregular spherical nanocrystals obtained in with H_2O_2 were about 10 and 20 nm in diameter, as shown in Fig. 4a. The rods were about 26 nm in diameter and 355 nm long, as shown in Fig. 4b, while the nanotubes were about 5nm in diameter and between 16 to 97 nm long. When HAc was used as a reaction medium, the diameters of the rods obtained without H_2O_2 were about 579 nm long (Fig. 4c and 4d). When IP was used as the reaction medium, the crystallite shapes turned into nanorods of different sizes and shapes. Once again, the mechanisms of crystal growth were influenced by the presence of the hydrogen peroxide. The effect of the presence or absence of hydrogen peroxide on the starting material can be explained by the same principle when isopropanol is used as a solvent. But when HAc is used as a solvent, the reaction medium behaves very differently. With the formation of gel, the titanium salt is not surrounded by OH^- ions and the nucleation of $Ti(OH)_x$ does not occur. After the addition of water, the titanium salt is surrounded by a large amount of OH^- that promotes a nucleation of $Ti(OH)_x$. Although the particle growth will be restricted by the surrounding OH^-, the slow formation of $Ti(OH)_x$ results in crystals of irregular shapes and sizes. As a result, large crystals are obtained, especially in the absence of H_2O_2.

Fig. 5 (a and b) shows the diffuse reflectance spectra of the anatase phase of titania. TiO_2 is an indirect semiconductor [KOFFYBERG et all., 1979] so that the band gap energy (Eg) of the samples can be determined from the tangent lines to the plots of the modified Kubelka-Munk function, $[F(R'\infty)hn]^{½}$, versus the energy of the exciting light [KIM et all., 1993].

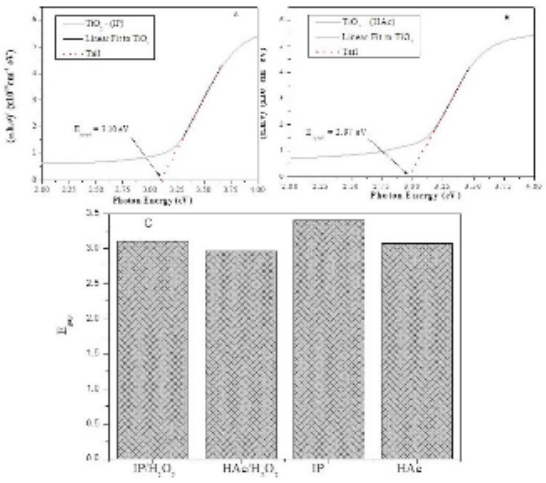

Figure 5. UV-vis absorbance spectra for TiO_2 (at room temperature) obtained in the presence of H_2O_2 using isopropanol ((a) - TiO_2-IP) or acetic acid ((b) - TiO_2-HAc) as reaction medium. And (c) Band gap energies for TiO_2 obtained in the presence and absence of H_2O_2 using isopropanol (IP) or acetic acid (HAc) as reaction medium.

As shown in Fig. 5c, the Eg values of TiO_2 were 3.10 and 2.97 eV for TiO_2 obtained in the presence of H_2O_2, in isopropanol (IP/H_2O_2) and acetic acid (HAc/H_2O_2), respectively. The band gaps obtained in this work are in line with data found in scientific literature [KUMAR; BADRINARAYANAN; SASTRY, ZHANG et all., 2007, CHOI et all., 2017] The absorption edge shifts towards shorter wavelengths for the TiO_2 obtained with HAc, which clearly indicates a decrease in the bandgap of the TiO_2 particles obtained with IP. The larger band gap of the TiO_2 - (IP) nanocrystals can be attributed to the quantum size effect. This is because the as-prepared TiO_2 - (IP) nanoparticles have a smaller crystalline size. The Eg values of TiO_2 obtained without H_2O_2 (Fig. 5c) were 3.07 and 3.40 eV, for TiO_2 obtained in IP and HAc, respectively

Fig. 6(a, b) shows the nitrogen adsorption–desorption isotherms of TiO_2 – (IP) and TiO_2 – (HAC) samples. It can be seen that both are type IV isotherms with a H1 hysteresis loop (according to IUPAC classification), which is a typical adsorption for mesoporous materials with one-dimensional cylindrical channels [SING et all., 1985].

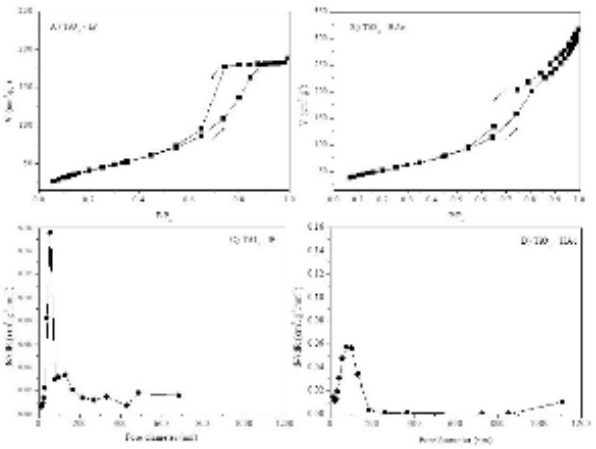

Figure 6. Adsorption-desorption N_2-isotherms (a and b) and pore size distribution (c and d) from TiO_2 obtained in the presence of H_2O_2 using isopropanol (a and c) or acetic acid (b and d) as reaction medium.

Furthermore, a well-defined step occurs at the relative pressure of 0.6–0.8, which indicates that the filling of the uniform mesopores is due to capillary condensation [GREGG; SING, 1982]. The position at which the inflection begins is clearly related to the pore size, and the sharpness of these steps indicates the uniformity of the mesopore size distribution [GREGG; SING, 1982]. The specific surface areas and pore parameters of the samples are summarized in Table 1. It can be seen that the TiO_2 – IP powder shows a large S_{BET} value of 192.8 $m^2\ g^{-1}$ and pore volume value of 0.46 $cm^3\ g^{-1}$. However, the specific surface area, porosity, and pore volume all decrease when the TiO_2 is obtained with HAc (see Table I). The pore size distribution curves obtained from the desorption branch of the nitrogen isotherm by the BJH (Barrett–Joyner–Halenda) method are shown in Fig. 8c and d. It can be seen that the TiO_2 – IP has an average pore size of 9.6 nm, and with TiO_2 – HAc, the average pore size is 7.4 nm.

The specific surface areas and pore parameters of the samples obtained without H_2O_2 are summarized in Table I. The TiO_2 – IP powder shows a high S_{BET} value of 148.7 $m^2\ g^{-1}$ and pore volume value of 0.22 $cm^3\ g^{-1}$.

The methylene blue (MB) decolorization experiments in water, presence of H_2O_2 and absence of light were conducted using TiO_2 as catalytic system Fig. 7.

Fig. 7 show evolution of decolorization of MB in the presence of several catalyst systems. TiO_2 obtained in HAc and presence of H_2O_2 was the better catalytic system. During incubation, approximately 50% of the MB was degraded in the presence of TiO_2-HAc (obtained in presence of H_2O_2) within 26min, and more than 90% decolorization was obtained in the presence within 2h. To investigate the effect of adding H_2O_2 well as well TiO_2 to the catalytic process of MB, two experiments were carried out: 1) MB in the presence of H_2O_2 and absence of TiO_2 and 2) MB in absence of H_2O_2 and TiO_2. No catalytic activity was observed.

Under the experimental conditions used in this study, we investigated the activity of TiO_2 obtained from Degussa (P25). Fig. 7 shown that in presence of P25 approximately 40% of MB was decolorized within 2h. All others TiO_2 systems reported in this work did not present significantly catalytic activity.

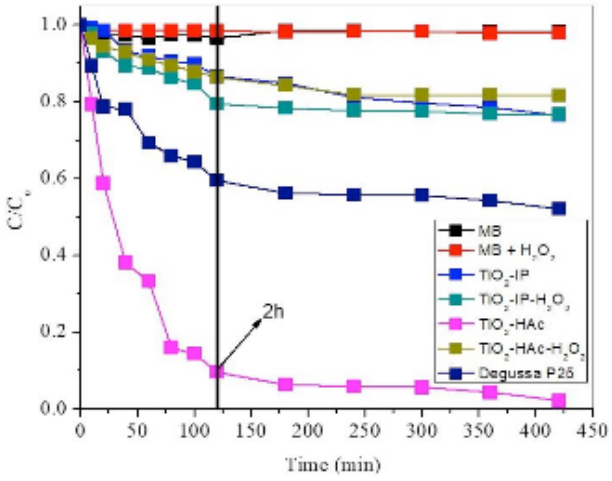

Figura 7. Decoloração do azul de metileno na presença de TiO_2 e H_2O_2.

4 I CONCLUSIONS

The following can be concluded from the results presented in this paper: a method for the preparation of TiO_2 nanoparticles with a large surface area and an exclusively anatase crystal structure has been demonstrated. The successful characterization of the synthesized particles revealed that the nanometer regime and the size of crystals were ~ 7 – 579 nm (~ 5 – 39 nm in diameter and ~16 – 579 in length), estimated using the Scherrer formula. This data is also supported by STEM micrograph evidence. The synthesized TiO_2 has a large surface area, 192 m^2/g as estimated by the BET method, which is an important property for catalytic, photocatalytic, and gas sensor applications. The particles showed a concomitant blue shift in the absorption spectra. The bandgap energy observed for different TiO_2 was 3.10 and 2.97 for TiO_2 obtained with IP and HAc, respectively, when H_2O_2 was used; and 3.07 and 3.40 for TiO_2 obtained with IP and HAc, respectively, when $H_2O_2$was not used. A TiO_2 catalyst was activated in a solution of H_2O_2, and the decolorization of methylene blue was improved in the presence of these pretreated particles. Decolorizing ratio of approximately 100% was obtained within 7h incubation period in the presence of TiO_2 obtained in HAc and presence of H_2O_2.

5 I ACKNOWLEDGEMENTS

Authors thankfully acknowledge to the CNPq and FAPEPI (Fundação de Amparo À Pesquisa do Piauí). The present work was supported by financial support from CNPq/FAPEPI (Proc. 304261/2009-2).

REFERENCES

AHMAD, M.S.; PANDEY, A.K.; RAHIM, N.A. **Advancements in the development of TiO_2 photoanodes and its fabrication methods for dye sensitized solar cell (DSSC) applications**. Renewable and Sustainable Energy Reviews v. 77, p. 89-108, 2017.

AHONEN, P.P.; TAPPER, U.; KAUPPINEN, E.I.; JOUBERT, J.C.; DESCHANVRES, J.L. **Aerosol synthesis of Ti–O powders via in-droplet hydrolysis of titanium alkoxide**. Materials Science and Engineering: A. v. 315, n. 1-2, p. 113-121, 2001.

ATTAR, A.S.; GHAMSARI, M.S.; HAJESMAEILBAIGI, F.; MIRDAMADI, S. **Synthesis and characterization of anatase and rutile TiO_2 nanorods by template-assisted method**. Journal of Materials Science v. 43, n. 17, p. 5924-5929, 2008.

BOKHIMI, X.; PEDRAZA, F. **Characterization of brookite and a new corundum-like titania phase synthesized under hydrothermal conditions**. Journal of Solid State Chemistry v. 177, n. 7, p. 2456-2463, 2004.

BORA, L.V.; MEWADA, R.K. **Visible/solar light active photocatalysts for organic effluent treatment: Fundamentals, mechanisms and parametric review**. Renewable and Sustainable Energy Reviews v. 76, p. 1393–1421, 2017.

CARP, O.; HUISMAN, C.L.; RELLER, A. **Photoinduced reactivity of titanium dioxide**. Progress in Solid State Chemistry v. 3, n. 1-2, p. 33-177, 2004.

CHANG, J.A.; VITHAL, M.; BAEK, I.C.; SEOK, S.I. **Morphological and phase evolution of TiO_2 nanocrystals prepared from peroxotitanate complex aqueous solution: Influence of acetic acid**. Journal of Solid State Chemistry 182 (2009) 749–756.

CHANG, J.A.; VITHAL, M.; BAEK, I.C.; SEOK. S.I. **Evolution of Phase and Morphology of Titanium Dioxide Induced from Peroxo Titanate Complex Aqueous Solution**. Journal of Nanoscience and Nanotechnology v. 10, n.1, p. 163–169, 2010.

CHOI, H.; KHAN, S.; CHOI, J.; DINH, D.T.T.; LEE, S.Y.; PAIK, U.; CHO, S-H.; KIM, S. **Synergetic control of band gap and structural transformation for optimizing TiO_2 photocatalysts**. Applied Catalysis B: Environmental v. 210, n. 5, p. 513–521, 2017.

DAIA, H.; CHENA, S.; LIA, Y.; ZENGA, B.; ZHANGA, S.; HONGB, Z.; LINA, Y. **Photoelectrochemical biosensor constructed using TiO_2 mesocrystals based multipurpose matrix for trypsin detection**. Biosensors and Bioelectronics v. 92, p. 687–694, 2017.

GAO, Y.; LUO, H.; MIZUSUGI, S.; NAGAI, M. **Surfactant-free Synthesis of Anatase TiO_2 Nanorods in an Aqueous Peroxotitanate Solution**. Crystal Growth and Design v. 8, n. 6, p. 1804–1807, 2008.

GAO, Y.; MASUDA, Y.; KOUMOTO, K. **Light-Excited Superhydrophilicity of Amorphous TiO_2 Thin Films Deposited in an Aqueous Peroxotitanate Solution**. Langmuir v. 20, n.8, p. 3188-3194, 2004.

GAO, Y.; MASUDA, Y.; PENG, Z.; YONEZAWA, T.; KOUMOTO, K. **Room temperature deposition of a TiO_2 thin film from aqueous peroxotitanate solution**. Journal of Materials Chemistry v. 13, p. 608–613, 2003.

GAO, Y.; NAGAI, M.; SEO, W-S.; KOUMOTO, K. **Template-free self-assembly of a nanoporous TiO_2 thin film**. Journal of the American Ceramic Society v. 90, n. 3, p. 831–837, 2007.

GARCIA-SEGURA, S.; BRILLAS, E. **Applied photoelectrocatalysis on the degradation of organic pollutants in wastewaters**. Journal of Photochemistry and Photobiology C Photochemistry Reviews v. 31, p. 1–35, 2017.

GOPAL, M.; CHAN, W.J.M.; DE JONGHE, L.C. **Room temperature synthesis of crystalline metal oxides**. Journal of Materials Science v. 32, n.22, p. 6001-6008, 1997.

GOUTAILLER, G.; GUILLARD, C.; DANIELE, S.; HUBERT-PFALZGRAF, L.G. Low temperature and aqueous sol–gel deposit of photocatalytic active nanoparticulate TiO_2. Journal of Materials Chemistry n. 13, p. 342-346, 2002.

GREGG, S.J.; SING, K.S.W. **Adsorption, Surface Area and Porosity**, 2d ed., Academic Press, London, p. 303, 1982.

HAO, H.; ZHANG, J. **Low temperature synthesis of crystalline mesoporous titania with high photocatalytic activity by post-treatment in nitric acid ethanol solution**. Materials Letter v. 63, n. 1, p. 106-108, 2008.

HIROSHI, M.; TAKEO, H.; YASUHIRO, S.H.; MAKOTO, E. **Hydrogen-sensing properties of anodically oxidized TiO_2 film sensors: Effects of preparation and pretreatment conditions**. Sensors Actuators B v. 108, n. 1-2, p. 467-472, 2005.

HU, Y.; TSAI, H.L.; HUANG, C.L. **Effect of brookite phase on the anatase–rutile transition in titania nanoparticles**. Journal European Ceramic Society v. 23, n. 5, p. 691-696, 2003.

JAGADALE, T.C.; TAKALE, S.P.; SONAWANE, R.S.; JOSHI, H.M.; PATIL, S.I.; KALE, B.B.; OGALE, S.B. **N-Doped TiO_2 Nanoparticle Based Visible Light Photocatalyst by Modified Peroxide Sol-Gel**

Method. Journal of Physics and Chemistry C v. 112, n. 37, p. 14595–14602, 2008.

KARTHIKEYAN, V.; MANIARASU, S.; MANJUNATH, V.; RAMASAMY, E.; VEERAPPAN, G. **Hydrothermally tailored anatase TiO_2 nanoplates with exposed {111} facets for highly efficient dye-sensitized solar cells**. Solar Energy v. 147 p. 202–208, 2017.

KIM, Y.I.; ATHERTON, S.J.; BRIGHAM, E.S.; MALLOUK, T.E. **Sensitized layered metal oxide semiconductor particles for photochemical hydrogen evolution from nonsacrificial electron donors**. Journal of Physics and Chemistry v. 97, n. 4 p. 11802-11809, 1993.

KOFFYBERG, F.P.; DWIGHT, K.; WOLD, A. **Research articleFull text access Interband transitions of semiconducting oxides determined from photoelectrolysis spectra**. Solid State Communications v. 30, n. 7, p. 433-437, 1979.

KUMAR, P.M.; BADRINARAYANAN, S.; SASTRY, M. **Nanocrystalline TiO_2 studied by optical, FTIR and X-ray photoelectron spectroscopy: correlation to presence of surface states**. Thin Solid Films v. 358, n. 1-2, p. 122-130, 2000.

LI, C.P.; WANG, J.F.; SU, W.B.; CHEN, H.C.; WANG, Y.J.; ZHUANG, D.X. **Effect of sinter temperature on the electrical properties of TiO_2-based capacitor–varistors**. Materials Letter v. 57, n. 8, p. 1400-1405, 2003.

LI, G.; PANG, S.; JIANG, L.; GUO, Z.; ZHANG, Z. Environmentally Friendly Chemical Route to Vanadium Oxide Single-Crystalline Nanobelts as a Cathode Material for Lithium-Ion Batteries. Journal of Physics Chemistry B v. 110, n. 19, p. 9383-9386, 2006.

LI, X.Z.; LI, H.; CHENG, L.F.; TONG, H.J. **Photocatalytic Oxidation Using a New CatalystTiO_2 Microsphere for Water and Wastewater Treatment**, Environmental Science and Technology v. 37, n.17, p. 3989-3994, 2003.

LI, Y.; WANG, S.; LEI, D.; HE, Y.; LI, B.; KANG, F. Acetic acid-induced preparation of anatase TiO_2 mesocrystals at low temperature for enhanced Li-ion storage. Journal of Materials Chemistry A v.5, p. 12236–12242, 2017.

LI, Y.; WHITE, T.; LIM, S.H. **Structure control and its influence on photoactivity and phase transformation of TiO_2 nano-particles**. Reviews on Advanced Materials Science v. 5, p. 211-215, 2003.

LIU, K.; ZHANG, M.; SHI, K.; ZHOU, W.; FU, H. **Uniform TiO_2 thin films with anatase nanocrystallites synthesized through evaporation-induced assembly**. Journal of Non-Crystalline Solids v. 352, n. 21-22, p. 2284-2287, 2006.

LOAN, T.T.; BANG, N.A.; HUONG, V.H.; LONG, N.N. **Effect of Cr^{3+} concentration on structural and optical properties of TiO_2:Cr^{3+}anatase and rutile phases**. Optical Materials v. 69, p. 30-37, 2017.

Michael, G. **Sol-Gel Processed TiO2 Films for Photovoltaic Applications**. Journal of Sol–Gel Science Technology v. 22, n. 1-2, p. 7-13, 2001.

MUHLEBACH, J.; MULLER, K.; SCHWARZENBACH, G. **The Peroxo Complexes of Titanium**. Inorganic Chemistry v.9, n.11, p. 2381–2390, 1970.

PACHECO, F.; GONZALEZ, M.; MEDINA, A.; VELUMANI, S.; ASCENCIO, J.A. **Structural analysis of cobalt titanate nanoparticles obtained by sol–gel process**. Applied Physics A: Materials Science and Processing v. 78, p. 531-536, 2004.

PARRA, R.; GÓES, M.S.; CASTRO, M.S.; LONGO, E.; BUENO, P.R.; VARELA, J.A. **Reaction Pathway to the Synthesis of Anatase via the Chemical Modification of Titanium Isopropoxide with Acetic Acid**. Chemistry of Materials v. 20, n.10, p. 143-150, 2008.

PUEYO, N.; MIGUEL, N.; MOSTEO, R.; OVELLEIRO, J.L.; ORMAD, M.P. **Synergistic effect of the presence of suspended and dissolved matter on the removal of cyanide from coking wastewater by TiO_2 photocatalysis**. Journal of Environmental Science and Health, Part A v. 52, n.2, p. 1–7, 2016.

SING, K.S.W.; EVERETT, D.H.; HAUL, R.A.W.; PIEROTTI, R.A. ROUQUEROL, J.; SIEMIENIEWSK, T. **Reporting physisorption data for gas/solid systems with special reference to the determination of surface area and porosity**. Pure Applied Chemistry v. 57, n. 4, p. 603-620, 1985.

SUGIMOTO, T.; ZHOU, X.; MURAMASTU, A. **Synthesis of uniform anatase TiO_2 nanoparticles by gel–sol method: 3. Formation process and size control**. Journal of Colloid Interface Science v. 259, n. 1, p. 43-52, 2003a.

SUGIMOTO, T.; ZHOU, X.; MURAMASTU, A. **Synthesis of uniform anatase TiO_2 nanoparticles by gel–sol method: 4. Shape control**. Journal of Colloid Interface Science v. 259, n. 1, p. 53-61, 2003b.

ZAKRZEWSKA, K.; RADECKA, M. **TiO_2-Based Nanomaterials for Gas Sensing—Influence of Anatase and Rutile Contributions**. Nanoscale Research Letter v. 12, n. 89, p. 1-8, 2017.

ZHANG, M.; XUE, T.; XU, S.; LI, Z.; YAN, Y.; HUANG, Y. **Adverse effect of substrate surface impurities on O_2 sensing properties of TiO_2gas sensor operating at high temperature**. Ceramics International v. 43, n. 7, p. 5842–5846, 2017.

ZHANG, S.; YU, Q.; CHEN, Z.; LI, Y.; YOU, Y. **Nano-TiO_2 particles with increased photocatalytic activity prepared by the miniemulsion method**. Materials Letter v. 61, n. 26, p. 4839-4842, 2007.

SOBRE O ORGANIZADORES

TAYRONNE DE ALMEIDA RODRIGUES: Filósofo e Pedagogo, especialista em Docência do Ensino Superior e Graduando em Arquitetura e Urbanismo, pela Faculdade de Juazeiro do Norte-FJN, desenvolve pesquisas na área das ciências ambientais, com ênfase na ética e educação ambiental. É defensor do desenvolvimento sustentável, com relevantes conhecimentos no processo de ensino-aprendizagem. Membro efetivo do GRUNEC - Grupo de Valorização Negra do Cariri. E-mail: tayronnealmeid@gmail.com ORCID: https://orcid.org/0000-0001-9378-1456

JOÃO LEANDRO NETO: Filósofo, especialista em Docência do Ensino Superior e Gestão Escolar, membro efetivo do GRUNEC. Publica trabalhos em eventos científicos com temas relacionados a pesquisa na construção de uma educação valorizada e coletiva. Dedica-se a pesquisar sobre métodos e comodidades de relação investigativa entre a educação e o processo do aluno investigador na Filosofia, trazendo discussões neste campo. Também é pesquisador da arte italiana, com ligação na Scuola de Lingua e Cultura – Itália. Amante da poesia nordestina com direcionamento as condições históricas do resgate e do fortalecimento da cultura do Cariri. E-mail: joaoleandro@gmail.com ORCID: https://orcid.org/0000-0003-1738-1164

DENNYURA OLIVEIRA GALVÃO: Possui graduação em Nutrição pela Universidade Federal da Paraíba, mestrado pela Universidade Federal do Rio Grande do Norte e doutorado em Ciências Biológicas (Bioquímica Toxicológica) pela Universidade Federal de Santa Maria (2016). Atualmente é professora titular da Universidade Regional do Cariri. E-mail: dennyura@bol.com.br LATTES: http://lattes.cnpq.br/4808691086584861

Agência Brasileira do ISBN
ISBN 978-85-7247-331-6